Published in final edited form as:

J Proteome Res. 2024 July 05; 23(7): 2608–2618. doi:10.1021/acs.jproteome.4c00338.

Proteomics Analysis of Interactions between Drug-Resistant and Drug-Sensitive Cancer Cells: Comparative Studies of Monoculture and Coculture Cell Systems

Zongkai Peng,

Department of Chemistry and Biochemistry, University of Oklahoma, Norman, Oklahoma 73019, United States

Nagib Ahsan*,

Department of Chemistry and Biochemistry, University of Oklahoma, Norman, Oklahoma 73019, United States; Mass Spectrometry, Proteomics and Metabolomics Core Facility, Stephenson Life Sciences Research Center, University of Oklahoma, Norman, Oklahoma 73019, United States

Zhibo Yang*

Department of Chemistry and Biochemistry, University of Oklahoma, Norman, Oklahoma 73019, United States

Abstract

Cell–cell interactions, which allow cells to communicate with each other through molecules in their microenvironment, are critical for the growth, health, and functions of cells. Previous studies show that drug-resistant cells can interact with drug-sensitive cells to elevate their drug resistance level, which is partially responsible for cancer recurrence. Studying protein targets and pathways involved in cell–cell communication provides essential information for fundamental cell biology studies and therapeutics of human diseases. In the current studies, we performed direct coculture and indirect coculture of drug-resistant and drug-sensitive cell lines, aiming to investigate intracellular proteins responsible for cell communication. Comparative studies were carried out using monoculture cells. Shotgun bottom-up proteomics results indicate that the P53 signaling pathway has a strong association with drug resistance mechanisms, and multiple TP53-related proteins were upregulated in both direct and indirect coculture systems. In addition,

*Corresponding Authors: **Nagib Ahsan** – Department of Chemistry and Biochemistry, University of Oklahoma, Norman, Oklahoma 73019, United States; Mass Spectrometry, Proteomics and Metabolomics Core Facility, Stephenson Life Sciences Research Center, University of Oklahoma, Norman, Oklahoma 73019, United States; nahsan@ou.edu, **Zhibo Yang** – Department of Chemistry and Biochemistry, University of Oklahoma, Norman, Oklahoma 73019, United States; zhibo.yang@ou.edu.

Supporting Information

The Supporting Information is available free of charge at https://pubs.acs.org/doi/10.1021/acs.jproteome.4c00338.

Figure S1, quality control of label-free quantitative proteomics; Figure S2, comparison between the monoculture drug-resistant and drug-sensitive cells; Figure S3, P53 signaling pathway and the highlighted proteins upregulated in drug-resistant cells; Figure S4, workflow of the direct coculture and indirect coculture; and Figure S5, upregulated HIF-1 signaling pathways and TCA cycle in indirect coculture cells (PDF)

All identified proteins and upregulated proteins in P53 pathways in monoculture and coculture cells (XLSX)

Volcano plot of proteins in monoculture and coculture cells (XLSX)

Enriched upregulated KEGG pathways in monoculture and coculture systems (XLSX)

The authors declare no competing financial interest.

Complete contact information is available at: https://pubs.acs.org/10.1021/acs.jproteome.4c00338

cell–cell communication pathways, including the phagosome and the HIF-signaling pathway, contribute to both direct and indirect coculture systems. Consequently, AK3 and H3–3A proteins were identified as potential targets for cell–cell interactions that are relevant to drug resistance mechanisms. We propose that the P53 signaling pathway, in which mitochondrial proteins play an important role, is responsible for inducing drug resistance through communication between drug-resistant and drug-sensitive cancer cells.

Graphical Abstract

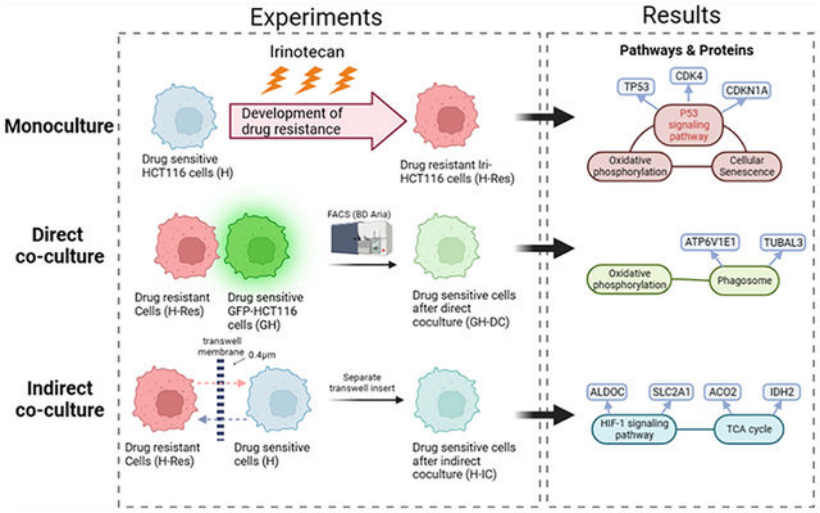

Keywords

drug resistance; cell–cell communication; quantitative proteomics; direct cell coculture; indirect cell coculture

INTRODUCTION

Cell–cell interactions play an important role in the development, homeostasis, and function of cells, and they influence multicellular organisms and diseases. These interactions enable communication among cells, allowing them to respond to changes in their microenvironment. Cell–cell interactions are of great interest for cancer research because they are critical in cancer cell progression, invasion, and metastasis. In cancer studies and treatments, the efficacy of chemotherapy is limited by the drug resistance of tumors, resulting in a treatment failure. Drug-resistant cells not only possess resistance by themselves but can facilitate drug-sensitive cells to increase their resistance to drugs through interactions in the microenvironment.[1–3] In-depth studies of chemoresistance induced by cell–cell interactions can help us to understand tumor recurrence mechanisms and improve clinical treatment strategies. However, the exact mechanisms of resistance in drug-resistant cells and cell–cell communication are not fully understood.[4]

To understand cell–cell communication, different mechanisms have been proposed. In respect of species involved in molecular transmission, secreted soluble molecules (e.g.,

growth factors[5] and estrogen[3]) and extracellular vesicles (e.g., exosomes[6]) have been reported. Regarding the interaction distance, both short-distance and long-distance cell–cell communication approaches have been proposed.[7–11] Accordingly, two different types of *in vitro* experimental models have been developed to study cell–cell communication affected by distances: indirect and direct coculture systems. In indirect coculture systems, cells are separated by different barriers (e.g., membranes[12]) or cultured in different containers,[13] whereas cell signaling molecules are transmitted through a shared culture medium. These coculture models can be used to mimic long-distance communication. These indirect coculture devices (e.g., Transwell) are commonly used for studies of cell–cell interactions primarily because of their commercial availability, ease-of-use, and excellent reproducibility. These indirect coculture systems are suitable to study certain long-distance communication but cannot effectively mimic short-distance communication. For example, intercellular transport proteins and RNA are distance-sensitive and even contact-dependent factors in actual vivid microenvironments.[14,15] Thus, direct coculture systems, in which different types of cells are cultured in the same device with direct cell–cell contact, have been developed to better mimic *in vivo* systems.

Although direct coculture systems possess unique advantages, the analysis of different types of cells in these systems requires cells to be distinguished or separated prior to analysis. To achieve this goal, both fluorescence-labeled (e.g., by fluorescent proteins or dyes) cells and regular (i.e., nonlabeled) cells are commonly used for direct coculture, whereas standard fluorescence-based techniques, e.g., fluorescence microscopy and fluorescence-assisted cell sorting (FACS), can be used to distinguish and separate different types of cells in the direct coculture systems.

We have recently established both direct and indirect coculture systems using drug-sensitive and drug-resistant HCT116 (human colorectal) cancer cell lines in which one of them was labeled with GFP. We then conducted single-cell mass spectrometry (SCMS) experiments to study the influence of drug-resistant cells on the metabolism of drug-sensitive cells. Our results indicated that drug-resistant cells facilitated the drug-sensitive cells to increase their drug resistance.[1,2,16] In addition, metabolites' profiles of drug-sensitive cells were changed (e.g., upregulated sphingomyelin lipids and lactic acid but downregulated TCA cycle intermediate[16]) after coculture. However, there is a lack of comprehensive understanding of proteins involved in cell–cell communication, particularly distance mediated interactions influencing drug resistance of cancer cells.[14] In addition, investigating protein targets responsible for the induction of drug resistance potentially provides a great opportunity to discover personalized anticancer drugs,[17] such as antibody–drug conjugates (ADCs), to combat drug resistance and cancer recurrence.

Here, we utilized the GFP-labeled and regular (unlabeled) HCT116 cell lines for both direct and indirect coculture systems for label-free quantitative mass spectrometry (MS) bottom-up proteomics studies (Figure 1). Our primary goal is to study intracellular target proteins involved in long-distance and short-distance cell–cell interactions that are responsible for elevated drug resistance. We are particularly interested in the influence of drug-resistant cancer cells on drug-sensitive cells, which gained increased drug-resistance through coculture with drug-resistant cells. We produced irinotecan (Iri)-resistant HCT116

cells (no GFP labeling) using our established protocols.[16] The Iri-resistant and regular (drug-sensitive) cells were subjected to both direct and indirect cocultures, followed by cell separation and bottom-up quantitative MS proteomics analyses. We discovered a series of proteins responsible for the facilitation of drug resistance in drug-sensitive cells through cell–cell communication. Our systematic proteomic analysis made it possible to find potential protein targets related to drug resistance mechanisms through cell–cell interactions, which might provide new inspiration for cancer treatment and clinical biomarker targets.

EXPERIMENTAL PROCEDURES

Monoculture System

Monoculture systems were prepared using four cell lines, including two drug-sensitive and two drug-resistant cell lines. Human colorectal cancer HCT116 (H) cells, which were used as the control cells, were purchased from the American Type Culture Collection (ATCC; Rockville, MD, USA). HCT116 cells were cultured at 37 °C with 5% CO_2 in Petri dishes using McCoy's 5A media supplemented with 10% FBS and 1% Pen Strep. HCT116-GFP (GH) cells, generated from HCT116 cells by lentiviral vector transduction, were purchased from Cellomics Technology (Halethorpe, MD, USA). Puromycin at 1 μg/mL was added to the complete growth medium to maintain the expression of green fluorescence protein in HCT116-GFP cells. Both H and GH were used as the drug-sensitive cell lines. Irinotecan (Iri) was used as the anticancer drug to generate drug-resistant cell lines (H-Res and GH-Res) by culturing their corresponding parental cells (H and GH) in the complete growth medium containing 1.0 μM Iri for 20 days. These drug-resistant cells were then cultured in drug-free complete medium for 4 days to deplete intracellular anticancer drug molecules. The medium was changed every 24 h during the depletion process.

Coculture System

Both indirect and direct coculture systems were prepared using one drug-resistant (H-Res) and one drug-sensitive cell line (i.e., H (for indirect coculture) or GH (for direct coculture)).

Indirect Coculture

A Corning Transwell insert (Costar, part no. 3450) and six-well plates (Costar, part no. 3516) were used for the indirect coculture. Cells in this indirect coculture model were separated by a 0.4 μm membrane, which allowed proteins and small molecules to be transferred through the membrane for communication without direct cell–cell contact between two cell lines. Briefly, 1.5 mL of H-Res cells (5×10^5 cells) were added into one Transwell insert, and 2.6 mL of H cells (1×10^5 cells) were added into a well of the 6-well plates. Then the inserts containing drug-resistant cells were combined with the 6-well plates containing drug-sensitive cells. After 72 h of incubation (at 37 °C with 5% CO_2), drug-sensitive cells were collected from the 6-well plates for preparation for bottom-up MS proteomics analysis. These drug-sensitive cells collected from the indirect coculture were referred to as H-IC.

Direct Coculture

GFP-labeled drug-sensitive cells (GH) and drug-resistant cells (H-Res) were directly cocultured in the same 6-well plates, allowing for direct cell–cell contact between two cell lines. Briefly, a mixture of 4 mL of cell culture medium containing GH (1×10^5) and H-Res (5×10^5) cells was added into a well in the 6-well plates and incubated for 72 h (at 37 °C with 5% CO_2). Then, after removing the culture medium and washing with Gibco Dulbecco's Phosphate Buffered Saline (DPBS, 14190–250, MilliporeSigma, Rockville, MD), Trypsin EDTA was added to detach the cells. Trypsinization was stopped by adding the complete medium (containing 10% FBS). Cells were transferred into a 1.5 mL LoBind tube (Sarstedt ref. 72.706.600, Nümbrecht, Germany), centrifuged at 500 g at 4 °C for 5 min, washed twice with DPBS, and stored on ice. FACS was used to isolate GH cells from direct coculture, which were referred to as GH-DC. Cells were washed twice with DPBS prior to protein extraction steps.

Cell Protein Extraction and Sample Preparation for Label-Free MS Proteomics Analysis

Cell protein extraction was performed following previously published protocols.[18] Briefly, 8.0 M urea solution was added to the cell pellet to extract and denature proteins. Protein concentration was measured at 280 nm using a NanoDrop One instrument (Thermo Fisher Scientific, IL, USA). For each group of cell lines, measurements of three biological replicates were performed. In total, 100 μg of protein was taken from each sample, and 1.0 μg of BSA (catalog no. 23225, Thermo Scientific, Waltham, MA) was spiked in as the internal standard. In-solution digestion was performed using Trypsin/Lys-C (catalog no. V5071, Promega, WI, USA). Peptides were desalted using a Waters C18 Sep-Pak cartridge (cat. no. WAT023590, Waters, Milford, MA, USA) and then dried using speed-vac (SVC 100H, Savant) for 8 h. Each sample was resuspended with 200 μL of mobile phase A (water with 0.1% FA). An equal amount (3.0 μL) of sample was injected into the LC-MS/MS analysis.

LC-MS/MS and Data Analysis

The LC-MS/MS analysis was performed according to our earlier published protocols[18] using a Dionex UltiMate 3000 UHPLC system (Thermo Fisher Scientific, CA, USA) connected to a Q Exactive HF-X mass spectrometer (Thermo Fisher Scientific, Waltham, MA). The resuspended tryptic peptides were loaded onto an in-house packed trap column (150 μm × 3 cm, packed with Bio-C18 3 μm resin, Sepax Technologies, DE, USA) using mobile phase A (0.1% formic acid in LC-MS grade water) at a flow rate of 3 μL/min for 10 min and separated on an analytical column (75 μm × 30 cm, packed in house with Bio-C18 3 μm resin, Sepax Technologies) at 350 nL/min. The total LC-MS/MS run time was 90 min including column washing and re-equilibration.

MS RAW files were searched against the UniProt reviewed human (TaxID: UP000005640) protein database using the Sequest algorithm within Proteome Discoverer v 2.4 (Thermo Fisher Scientific, San Jose, CA). The Sequest database search was performed with the following parameters: trypsin enzyme cleavage specificity, two possible missed cleavages, 10 ppm mass tolerance for precursor ions, and 0.02 Da mass tolerance for fragment ions. Search parameters permitted dynamic modification of methionine oxidation (+15.9949

Da) and static modification of carbamidomethylation (+57.0215 Da) on cysteine. Peptide assignments from the database search were filtered down to a 1% FDR (false discovery rate). Label-free quantitation across the samples employed the Minora algorithm and the adjoining bioinformatics tools available in Proteome Discoverer. A 1.5-fold increase or decrease in abundance with a p-value < 0.05 was considered statistically significant.

ELISA (Enzyme-Linked Immunosorbent Assay)

To verify functional proteins detected in LC-MS/MS experiments, ELISA verification of two selected proteins (adenylate kinase 3 (AK3) and H3 histone 3A (H3–3A)) was performed for both drug-resistant cells (H-Res) and drug-sensitive cells (H and GH) from monoculture systems. Antibodies of AK3 (RDR-AK3-Hu, Reddot Biotech, Houston, TX) and H3–3A (abx387828, Abbexa, Sugar Land, TX) were used to quantify their corresponding cellular proteins, following the protocols provided by their vendors. Briefly, 1×10^5 drug-sensitive (H and GH) or 5×10^5 drug-resistant (H-Res) cells were seeded in 6-well plates. After 72 h of culture, cells were detached, washed twice using DPBS, and then lysed with 100 μL of 8.0 M urea. Following protocols from the manufacturers, 300 μL of dilution buffer from the kit (additional 300 μL DPBS was added for AK3 measurements) were added in cell lysates prior to the quantification steps. Protein concentration was measured using a NanoDrop One (Thermo Fisher Scientific, Waltham, MA). Each sample was analyzed in triplicate, and standard curves were generated with GraphPad Prism. AK3 and H3–3A concentrations were normalized to the total protein concentration for a fair comparison.

Bioinformatics

All functional and pathway analyses were performed using the ShinyGO 0.77 bioinformatics platform.[19] Heatmaps and volcano plots were plotted by SRplot (https://www.bioinformatics.com.cn/en), a free online platform for data analysis and visualization. Protein–protein interaction analysis of changed proteins was searched through STRING 12.0 (https://string-db.org/).[20] The potential protein pathway was searched through KEGG[21–23] (https://www.genome.jp/kegg/pathway.html). A Venn diagram was generated using Molbiotools (https://molbiotools.com/listcompare.php). An abstract graph and P53 pathway graph were generated using Biorender (https://www.biorender.com/). All the bar plots was generated with GraphPad Prism version 7.0 for Windows, GraphPad Software, Boston, Massachusetts USA (https://www.graphpad.com). The remaining parts were generated by Microsoft PowerPoint and Excel 365.

RESULTS

In this study, we prepared both mono- and coculture models using drug-sensitive cells and drug-resistant cells. We then performed global MS proteomics studies of cells to understand cell–cell communication (Figure 1). GFP-labeled cells were used in coculture systems to discriminate different cell types. It is known that GFP labeling has no significant influence on metabolism and functions of cells.[24] In addition, our previous studies show that GFP labeling has no significant influence on the drug resistance of cancer cells.[16] To generate drug-resistant cells, irinotecan (Iri, CPT-11) was used to treat drug-sensitive cells (H and GH) for 20 days. In most studies, drug-resistant cancer cells are produced using gradually

increasing doses of anticancer drugs for relatively long treatment times (e.g., for 6–12 months or longer), whereas limited studies have been performed to investigate cells with early stage drug resistance.[25] Irinotecan is a potent anticancer drug used in the first-line therapy of advanced colorectal cancer, and its activated CPT-11 form, SN-38, binds to topoisomerase 1 and stops DNA replication. Our previous studies indicated that these 20-day resistant cells (H-Res) acquired 5.72-fold increased drug resistance levels compared with their parental cells.[25–27]

A total of six cell lines were obtained from the mono- and coculture systems, including drug-sensitive (H and GH) and drug-resistant (H-Res and GH-Res) cells in monocultures as well as drug-sensitive cells in indirect (H-IC) and direct coculture (RH-DC) with the drug-resistant cell line. A total of 2,542 and 1,983 unique protein groups were successfully identified and quantified in monoculture and coculture systems, respectively. Comprehensive data analyses, including principal component analysis (PCA), heat map clustering, volcano plot illustration, and protein pathway analysis (using KEGG), were performed for all identified proteins.

Proteome Profiling of Monoculture Cells

In total, 12 samples (i.e., three analytical replicates from each of monocultured cell groups (H, GH, H-Res, and GH-Res) were analyzed, and 2,542 unique protein groups were successfully identified and quantified. Proteins' quantities were normalized. The sequence coverage of spiked BSA (1 μg of BSA/100 μg of proteins) is higher than 82% in all monoculture samples, indicating efficient peptide trypsin digestion and sensitive MS detection (Figure S1). The relative abundances of BSA were compared among different groups of cell samples, and a small standard deviation suggests that the same protein in different groups was accurately quantified for a fair comparison (Figure S1).

PCA was used to illustrate the overall profiles of all identified proteins (with normalized abundances by peak areas) from different cell groups. A reasonably good reproducibility among the three analytical replicates was observed (Figure 2A). The influence on GFP labeling on protein expression can be also evaluated using PCA plots. By comparing protein profiles of paired GFP-labeled and nonlabeled cells, it is shown that, compared with the differences between drug-sensitive and drug-resistant cells, GFP labeling has no significant influence on the overall protein expression in drug-sensitive (H vs GH) and drug-resistant (H-Res vs GH-Res) cells (Figure 2A). Thus, GFP-labeled cells are suitable models for both drug-sensitive and drug-resistant cells in coculture systems.

Using PCA, significant differences were observed between the drug-sensitive and drug-resistant cells (i.e., H vs H-Res and GH vs GH-Res) in the monoculture systems (Figure 2A). Similarly, the heat map further demonstrated that clustered proteins with differential abundance were observed between the drug-sensitive and drug-resistant cells (Figure 2B). Volcano plots were utilized to illustrate proteins with significant upregulation or downregulation (with fold change > 1.5 or < 0.66, adjusted p-value < 0.05). A total of 159 proteins were significantly upregulated, whereas 55 proteins were downregulated in the drug-resistant group (H-Res) compared with the drug-sensitive (H) group (Figure 2B). We also compared the proteins between GFP-labeled and nonlabeled cells. For drug-

sensitive cell lines, 101 and 27 proteins were significantly upregulated and downregulated, respectively, in GH cells compared with H cells. For drug-resistant cell lines, 72 and 46 proteins were upregulated and downregulated, respectively, in the H-Res group compared with the GH-Res group (Figure S2D). Comparative studies were also carried out between drug-resistant and drug-sensitive cells: the abundances of 255 proteins increased and 93 proteins decreased in the GH-Res group compared with the H group (Figure S2B). These dysregulated proteins are likely related to both GFP expression and enhancement of drug resistance.

KEGG pathway analysis was performed for significantly upregulated proteins (>1.5-fold change and p-value < 0.05) in the Iri-resistant group (H-Res) compared to control group (H) (Figure 2D). To further understand protein–protein interactions among significantly upregulated proteins, STRING was used to illustrate the protein network for those involved in oxidative phosphorylation, cellular senescence, and the P53 signaling pathway (Figure 2E). The P53 signaling pathway is a key network that prevents gene mutations. P53 stabilizes genes in cells by interacting with multiple signal transduction pathways that affect cellular processes such as DNA repair and replication. It is known that TP53-related proteins are related to induced drug resistance.[28] The abundances of multiple P53 signaling pathway proteins (e.g., RRM2B, CYCS, SERPINB5, CDK1A, and CDK4) were significantly increased (Figure S3) in drug-resistant cell lines (H-Res and GH-Res) compared with their control groups (H and GH), indicating a strong association of P53 signaling pathways (Figure 2F) in the Iri resistance mechanisms.

Proteome Profiling of Direct and Indirect Coculture Cells

Our studies are focused on the influence of drug-resistant cells on drug-sensitive cells through cell–cell interactions. Thus, only drug-sensitive cells in the direct coculture (GH-DC) and indirect coculture (H-IC) were collected. In total, 1,983 proteins (<1% FDR) were successfully identified and quantified in GH-DC and H-IC cells. We then determined proteins with significantly changed abundances (fold change > 1.5 or < 0.66, p-value < 0.05). A total of 296 (253 upregulated and 43 downregulated) (Figure 3A) and 158 (58 upregulated and 100 downregulated) (Figure 3E) proteins were significantly changed in the direct (GH-DC) and indirect coculture (H-IC) models, respectively. Interestingly, some proteins (e.g., SRP14 and ECHDC1) showed coculture-specific alternation, i.e., they were not detected in monoculture systems, suggesting that they are relevant to the acquisition of drug resistance through cell–cell communication.

Direct Coculture Cell System

GFP-labeled drug-sensitive cells (GH-DC) were isolated from the direct coculture system containing drug-resistant cells (H-Res) (Figure S4A) using FACS. Drug-resistant cells (H-Res) can interact with the drug-sensitive cells (GH) through cell–cell contact and cell–matrix interactions in the direct coculture system, allowing the drug-sensitive cells to change their protein profiles and construct new pathways with elevated drug resistance. The volcano plot illustrated 253 upregulated and 43 downregulated proteins in GH-DC cells compared to the control (GH) (Figure S4B). Similar to that observed in the Iri-resistant cells (H-Res), Reactome pathway analysis of the upregulated proteins revealed that the

oxidative phosphorylation pathway was also upregulated in direct coculture cells (GH-DC). This pathway has a strong association with P53 signaling pathways (Figure 3B). GH-DC cells also activated transcriptional regulation by TP53 pathways, and the relevant proteins (MBD3, HDAC1, CARM1, NPM1, PPP2R1B, RFC3, RFC2, RFC5, and TNRSF10A) were upregulated (Figure 3C). These results indicate that transcriptional regulation by TP53 is important for drug-sensitive cells to gain drug resistance from drug-resistant cells through direct coculture. In particular, upregulated TNFRSF10A (DR4),[29] a surface receptor in tumor cells, indicates that this protein is likely a target for cell–cell communication (Figure 3D). In addition, the phagosome pathway was upregulated, and multiple relevant proteins (e.g., LAMP2, ATP6 V1E1, TUBAL3, TUBB3, TUBB6, and TUBB8) were overexpressed (Figure 3B).

Indirect Coculture Cell System

Drug-sensitive cells (H-IC) were harvested from the Transwell device used in an indirect coculture with drug-resistant cells (H-Res) (Figure 3F). A membrane (0.4 μm pore size) separated these two different types of cells, whereas molecular species can be transported for only cell–matrix (including metabolites, proteins, and hormone[30]) interactions without cell–cell contact, allowing cells to gain enhanced drug resistance. A total of 58 proteins were upregulated, whereas 100 proteins were down-regulated in the H-IC cells (Figure 3E). Multiple pathways (e.g., citrate cycle (TCA cycle) and HIF-1 signaling pathway) were upregulated (Figure 3F). Among them, ALDOA and ALDOC, which play significant roles in glycolysis and fructolysis steps for synthesis of ATP through TCA cycle,[31] were upregulated in the HIF- 1 signaling pathway, resulting in a reduced oxygen consumption process (Figures 3F and S5).

Similar to the trend observed from the direct coculture cells (GH-DC), the TP53-related protein–protein network was found to correlate with the interactions with drug-resistant cells in the indirect coculture cells. In H-IC cells, the upregulated proteins, including membrane glucose transporter (SLC2A1), isocitrate dehydrogenase (NADP(+)) 2 (IDH2), and histone proteins (H1–0, H4C1, and H3–3A), were directly related to TP53 proteins (Figures 3G and 3H).

Potential Protein Targets in Drug Resistance and Cell–Cell Communication

In this study, the P53 signaling pathway was found to be upregulated and strongly correlated with drug resistance mechanisms in Iri-resistant cells (Figures 2D and 2F). As the common proteins relevant to Iri resistance, AK3 and H3–3A were significantly upregulated in monoculture (H-Res), indirect coculture (H-IDC), and direct coculture (GH-DC) (Figure 4A). Overexpressed AK3 and H3–3A in coculture cells indicates that Iri resistance can be induced through molecular transfer during cell–cell communication.

To verify results obtained from label-free MS quantitative proteomics experiments, ELISA experiments were carried out for two selected proteins (H3–3A and AK3). Similar to MS results, ELISA measurements provided the same trends: both H3–3A and AK3 proteins were highly expressed in drug-resistant cells (H-Res) compared with control groups (H and GH) (Figures 4B and 4C). The AK3 protein, a GTP:ATP phosphotransferase present

in the mitochondrial matrix, is responsible for purine homeostasis. AK3 is directly related to both P53 (via RRM2B proteins) and oxidative phosphorylation pathways (Figure 2E), and the latter was also upregulated in direct coculture systems (Figure 2D), indicating AK3 is a potential biomarker for cell–cell communication of drug resistance. Multiple histones, including H3–3A, H1–0, and H4C1, are directly associated with TP53 proteins. These histones were upregulated in indirect coculture cells (GH-DC) (Figure 3G), contributing to the induced drug resistance through indirect interactions with drug resistance associated with the P53 signaling pathways.

DISCUSSION

Drug Resistance Related Mechanisms Observed in Monoculture Systems

Our previous studies indicated that the drug resistance level of HCT116 cells (H; IC_{50} = 2.90 ± 0.1 μM) can be significantly enhanced (H-IC; IC_{50} = 10.7 ± 1.9 μM) through indirect coculture with 20-day Iri-resistant HCT116 cells (H-Res; IC_{50} = 16.6 ± 1.4 μM).[16] In addition, numerous lipids, including ceramides and sphingolipids, were significantly upregulated.[32] In the current studies, we observed that several proteins associated with the sphingolipid signaling pathway (e.g., *N*-acylsphingosine amidohydrolase 1 (ASAH1) and ceramide synthase 2 (CERS2)) were abundant in Iri-resistant cell lines. ASAH1 gene-encoded protein catalyzes the degradation of ceramide and fatty acids, whereas CERS2 catalyzes the synthesis of very long acyl chain ceramides. It has been reported that radiation leads to ASAH1 overexpression in glioblastoma cells;[33,34] thus, inhibiting the activity of ASAH1 results in glioblastoma cell death.[35] These studies suggest that the ASAH1 protein is relevant to the development of radioresistance and recurrency of glioblastoma. Similarly, CERS2 expression is correlated to the degree of recurrence of numerous cancers.[36] Because ASAH1 and CERS2 affect the synthesis of sphingolipids and ceramides, the production of these lipids is likely critical for cells to establish resistance to the anticancer drug Iri. In fact, our previous studies indicate that a large number of ceramides and sphingolipids were upregulated in drug-resistant cells and cells cocultured with drug-resistant cells.[16] Thus, we have experimental evidence from both proteomics and metabolomics studies to demonstrate that the regulation of sphingolipids and ceramides is related to drug resistance.

As we previously demonstrated, cell-cycle arrest, senescence, and apoptosis are the three main outcomes of P53 activation.[37] Cell-cycle arrest allows cell repair and recovery from the stress (i.e., drug treatment) so that cell survival occurs, and resistance is gained. As observed in the monoculture systems, the P53 signaling pathway and relevant proteins, including cyclin-dependent kinase 4 (CDK4), cyclin-dependent kinase inhibitor 1A (CDKN1A), and cytochrome c (CYCS), were significantly upregulated in drug-resistant cells (Figures 2C and 3S). CDK4 affects the cell cycle pathway by progressing it from the G1 to the S phase, in which DNA synthesis occurs.[38] CDK4 is upregulated in multiple tumors, and its hyperactivity leads to drug resistance. In contrast, suppressing the expression or activity of CDK4 by its inhibitors (e.g., palbociclib, ribociclib, and abemaciclib[39]) is regarded as an effective strategy for cancer treatment.[40,41] CYCS is among proteins (>300) involved in the oxidative phosphorylation processes. These proteins are encoded by nuclear and mitochondrial genes, demonstrating that mitochondria play a key role

during the drug resistance mechanism.[42] Increased CYCS is correlated with drug resistance and poor survival of cancer (e.g., lymphoma[43]). Thus, it is not surprising that several proteins associated with the P53 pathway, including TP53I3, CDKN1A, CDK4, CYCS, and SERPINB5 proteins, were increased in resistant cells (H-Res and GH-Res). This provides the drug-resistant cells with a better chance to survive after treatment.

We also observed other potential pathways related to Iri resistance. For example, propanoate metabolism governs propionic acid metabolism, which is enriched in metastatic tumors to increase metastatic aggressiveness.[44] Multiple proteins involved in the propanoate metabolism pathway were identified in Iri-resistant cells, indicating that they are correlated with the drug-resistance mechanism. These proteins include the hydroxyacyl-CoA dehydrogenase alpha subunit (HADHA), the cytosolic enzyme ethylmalonyl-CoA decarboxylase (ECHDC1), and 3-hydroxyisobutyryl-CoA hydrolase (HIBCH). It has been reported that HADAH is overexpressed in cisplatin-resistant cancer cells.[45] ECHDC1 is one of the side products of acetyl-CoA carboxylase.[46] The expression of ECHDC1 is significantly increased in the gemcitabine-resistant cells.[47] High expression of HIBCH is correlated with poor survival in patients with colorectal cancer.[48]

Short-Distance Communication

Cell–cell communication can be classified into four types: autocrine signaling (secreted signaling molecules bind to the same cell), paracrine signaling (secreted signaling molecules act on nearby cells), endocrine signaling (secreted signaling molecules are carried through the circulation to act on distant cells), and juxtacrine (signaling processes require close contact).[30] According to the distance of molecular transfer between cells, cell–cell communication can be classified as short- and long-distance communication.[7] In the short-distance communication, cells communicate with each other by sending and accepting signal molecules (e.g., ligands, nitric oxide, and *P*-glycoproteins[49]) over short distances or through physical contact. The *in vitro* direct coculture systems are regarded as vivid models mimicking short-distance communication (i.e., paracrine and juxtacrine signaling) in *in vivo* microenvironments. Our previous studies showed that drug-sensitive cells gained drug resistance after being cocultured with drug-resistant cells through cell–cell and cell–matrix communication. Cell metabolites and related pathways were significantly changed (i.e., upregulated lactic acid and downregulated TCA cycle intermediate) after coculture.[16] Our current work indicates that the expression of some proteins relevant to Iri resistance (e.g., SRP14 and ECHDC1) were altered only in cocultured cells (H-IC and GH-DC), suggesting that the induction of drug resistance was through cell–cell communication.

We have observed multiple pathways that likely contribute to short-distance communication in direct coculture models. For example, phagosome and oxidative phosphorylation pathways were significantly upregulated in the direct coculture system (Figure 3B). In the phagosome process, upregulated vacuolar adenosine triphosphatases (V-ATPases), including ATP6 V1V1 and ATP6 V1G1, enhance drug resistance of cancer cells by reducing anticancer drug uptake or trapping drug molecules in acidic vesicles.[29,50]

Using Reactome pathway analysis of results obtained from direct coculture cells (GH-DC), we also discovered that tumor protein 53 (TP53) and tumor necrosis factor receptor

superfamily member 10A (TNFRSF10A) were upregulated (Figure 3D). In fact, multiple upregulated proteins, including AK3, H3–3A, and TNFRSF10A, have direct relations with the TP53 protein, indicating the importance of P53 signaling pathways in direct coculture systems through short-distance communication.

Long-Distance Communication

In long-distance communication, cells usually send signaling molecules using circulatory systems such as the bloodstream. For *in vitro* models, a physical barrier (i.e., membrane) is needed to mimic this endocrine signaling. The indirect coculture model used in the current work involves culturing two types of cells (i.e., drug-sensitive and drug-resistant cells) in the same culture medium, whereas these types of cells were separated by using a Transwell (0.4 μm membrane) device. After 72 h of indirect coculture, our results indicated that the TCA cycle, which plays an important role in drug resistance development,[51] was significantly upregulated in the drug-sensitive cells. The IC_{50} data shows that the IC_{50} value of the sensitive cells increases three times after indirect coculture (H-IC, 10.7 μM vs H, 2.9 μM), indicating an effective transfer of resistance to the sensitive cells.[16] In addition, Aconitase 2 (ACO2), which is a protein that catalyzes the interconversion of citrate to isocitrate in the TCA cycle, was upregulated (Figure 2 H). According to previous studies, ACO2 is a potential immunotherapeutic biomarker for multiple cancer types, including colon carcinoma.[52] Associated with the TCA cycle, hypoxia-inducible factor 1 (HIF-1) was also upregulated (Figure 2F). HIF-1 is responsible for sensing and adapting the cellular response to oxygen availability. This indicates the Warburg effect and shows that cells have an increased glycolysis activity. Eventually, the proteins encoded by the HIF-1 gene increase O_2 delivery, enabling cells to adapt to O_2 deprivation. As observed in multiple human cancers, activation of HIF-1 signaling increases multidrug resistance by enhancing the proliferation, invasion, and migration of tumor cells.[53] In the HIF-1 signaling pathway, glucose transporter member 1 GLUT1 (SLC2A1), a glucose transporter on the cell membrane controlling glucose concentration, was found to be highly upregulated after indirect coculture (Figure 2H). Previous studies indicate that SLC2A1 is highly expressed in many cancers.[54] In addition, we have observed other upregulated proteins, such as isocitrate dehydrogenase [NADP] IDH2 and histone proteins (e.g., H3–3A), directly related to the TP53 protein in this indirect protein–protein interaction network.

CONCLUSION

Overall, we studied intracellular proteins involved in cell–cell communication in two coculture models (indirect and direct cocultures) using drug-sensitive cells (i.e., HCT116 and HCT116GFP) and drug-resistant cells (i.e., IRI-HCT116 and IRI-HCT116-GFP). Label-free bottom-up shotgun proteomics results show that the P53 signaling pathway has a strong association with Iri drug resistance mechanisms. It is fascinating that P53 signaling pathway proteins were upregulated in both direct and indirect coculture systems, indicating that P53 contributes to the facilitation of drug resistance in drug-sensitive cells through their communication with drug-resistant cells. Upregulated pathways (e.g., oxidative phosphorylation) were observed in both direct coculture and drug-resistant cells, showing that they have a strong association with short-distance communication activities and

could be the potential pathway of the Iri resistance mechanism. As for the long-distance communication model, the energy-related TCA cycle and HIF signaling pathways were upregulated in indirect coculture systems. We propose protein targets (e.g., AK3 and H3–3A) contribute to cell–cell communication for drug-resistance information; by inhibiting these proteins, it may slow down recurrence for colon cancer Iri treatments. Our current studies are focused on the analysis of intracellular proteins in drug-sensitive cancer cells affected by drug-resistant cancer cells through cell–cell communications. Although extracellular species (e.g., growth factors and extracellular vesicles) are critical for cell–cell communication, these studies are beyond the scope of the current work.

Supplementary Material

Refer to Web version on PubMed Central for supplementary material.

ACKNOWLEDGMENTS

This work was supported by funds from National Science Foundation (2305182), the National Institutes of Health (1R01AI177469), and the University of Oklahoma's Office of the Vice President for Research and Partnerships.

Data Availability Statement

Proteomics data can be found at the MassIVE database via MSV000092944.

REFERENCES

(1). Brücher BL; Jamall IS Cell-cell communication in the tumor microenvironment, carcinogenesis, and anticancer treatment. Cellular Physiology and Biochemistry 2014, 34 (2), 213–243. [PubMed: 25034869]

(2). Frankfurt OS; Seckinger D; Sugarbaker EV Intercellular transfer of drug resistance. Cancer Research 1991, 51 (4), 1190–1195. [PubMed: 1997161]

(3). Emond R; Griffiths JI; Grolmusz VK; Nath A; Chen J; Medina EF; Sousa RS; Synold T; Adler FR; Bild AH Cell facilitation promotes growth and survival under drug pressure in breast cancer. Nat. Commun 2023, 14 (1), 3851. [PubMed: 37386030]

(4). Housman G; Byler S; Heerboth S; Lapinska K; Longacre M; Snyder N; Sarkar S Drug resistance in cancer: an overview. Cancers 2014, 6 (3), 1769–1792. [PubMed: 25198391]

(5). Korkaya H; Liu S; Wicha MS Breast cancer stem cells, cytokine networks, and the tumor microenvironment. J. Clin. Invest 2011, 121 (10), 3804–3809. [PubMed: 21965337]

(6). Lindoso RS; Collino F; Vieyra A Extracellular vesicles as regulators of tumor fate: crosstalk among cancer stem cells, tumor cells and mesenchymal stem cells. Stem Cell Investigation 2017, 4 (9), 75–75. [PubMed: 29057247]

(7). Vis MA; Ito K; Hofmann S Impact of culture medium on cellular interactions in in vitro co-culture systems. Frontiers in bioengineering and biotechnology 2020, 8, 911. [PubMed: 32850750]

(8). Pandurangan M; Hwang I Application of cell co-culture system to study fat and muscle cells. Applied microbiology and biotechnology 2014, 98, 7359–7364. [PubMed: 25038928]

(9). Kuppusamy P; Kim D; Soundharrajan I; Hwang I; Choi K Adipose and Muscle Cell Co-Culture System: A Novel In Vitro Tool to Mimic the In Vivo Cellular Environment. Biology 2021, 10, 6.

(10). Goers L; Freemont P; Polizzi KM Co-culture systems and technologies: taking synthetic biology to the next level. Journal of The Royal Society Interface 2014, 11 (96), No. 20140065. [PubMed: 24829281]

(11). Borciani G; Montalbano G; Baldini N; Cerqueni G; Vitale-Brovarone C; Ciapetti G Co–culture systems of osteoblasts and osteoclasts: Simulating in vitro bone remodeling in regenerative approaches. Acta biomaterialia 2020, 108, 22–45. [PubMed: 32251782]

(12). Li W; Khan M; Mao S; Feng S; Lin J-M Advances in tumor-endothelial cells co-culture and interaction on microfluidics. Journal of Pharmaceutical Analysis 2018, 8 (4), 210–218. [PubMed: 30140484]

(13). Renaud J; Martinoli M-G Development of an insert co-culture system of two cellular types in the absence of cell-cell contact. JoVE (Journal of Visualized Experiments) 2016, 113, No. e54356.

(14). Bogdanowicz DR; Lu HH Studying cell-cell communication in co-culture. Biotechnology journal 2013, 8 (4), 395. [PubMed: 23554248]

(15). Heng BC; Cao T; Lee EH Directing stem cell differentiation into the chondrogenic lineage in vitro. Stem cells 2004, 22 (7), 1152–1167. [PubMed: 15579636]

(16). Chen X; Peng Z; Yang Z Metabolomics studies of cell–cell interactions using single cell mass spectrometry combined with fluorescence microscopy. Chemical Science 2022, 13 (22), 6687–6695. [PubMed: 35756524]

(17). An Y; Zhou L; Huang Z; Nice EC; Zhang H; Huang C Molecular insights into cancer drug resistance from a proteomics perspective. Expert review of proteomics 2019, 16 (5), 413–429. [PubMed: 30925852]

(18). Ahsan N; Fornelli L; Najar FZ; Gamagedara S; Hossan MR; Rao RSP; Punyamurtula U; Bauer A; Yang Z; Foster SB; et al. Proteomics evaluation of five economical commercial abundant protein depletion kits for enrichment of diseases-specific biomarkers from blood serum. Proteomics 2023, 23, No. 2300150.

(19). Ge SX; Jung D; Yao R ShinyGO: a graphical gene-set enrichment tool for animals and plants. Bioinformatics 2020, 36 (8), 2628–2629. [PubMed: 31882993]

(20). Szklarczyk D; Kirsch R; Koutrouli M; Nastou K; Mehryary F; Hachilif R; Gable AL; Fang T; Doncheva NT; Pyysalo S; Bork P; Jensen LJ; von Mering C The STRING database in 2023: protein-protein association networks and functional enrichment analyses for any sequenced genome of interest. Nucleic Acids Res. 2023, 51 (D1), D638–d646. [PubMed: 36370105]

(21). Kanehisa M Toward understanding the origin and evolution of cellular organisms. Protein Sci. 2019, 28 (11), 1947–1951. [PubMed: 31441146]

(22). Kanehisa M; Furumichi M; Sato Y; Kawashima M; Ishiguro-Watanabe M KEGG for taxonomy-based analysis of pathways and genomes. Nucleic Acids Res. 2023, 51 (D1), D587–d592. [PubMed: 36300620]

(23). Kanehisa M; Goto S KEGG: kyoto encyclopedia of genes and genomes. Nucleic Acids Res. 2000, 28 (1), 27–30. [PubMed: 10592173]

(24). Yang J; Wang N; Chen D; Yu J; Pan Q; Wang D; Liu J; Shi X; Dong X; Cao H The impact of GFP reporter gene transduction and expression on metabolomics of placental mesenchymal stem cells determined by UHPLC-Q/TOF-MS. Stem cells international 2017, 2017, 1.

(25). McDermott M; Eustace AJ; Busschots S; Breen L; Crown J; Clynes M; O'Donovan N; Stordal B In vitro development of chemotherapy and targeted therapy drug-resistant cancer cell lines: a practical guide with case studies. Frontiers in oncology 2014, 4, 40. [PubMed: 24639951]

(26). Biedler JL; Spengler BA Reverse transformation of multidrug-resistant cells. Cancer and Metastasis Reviews 1994, 13, 191–207. [PubMed: 7923550]

(27). Liu R; Sun M; Zhang G; Lan Y; Yang Z Towards early monitoring of chemotherapy-induced drug resistance based on single cell metabolomics: Combining single-probe mass spectrometry with machine learning. Anal. Chim. Acta 2019, 1092, 42–48. [PubMed: 31708031]

(28). Hientz K; Mohr A; Bhakta-Guha D; Efferth T The role of p53 in cancer drug resistance and targeted chemotherapy. Oncotarget 2017, 8 (5), 8921–8946. [PubMed: 27888811]

(29). Stransky L; Cotter K; Forgac M The Function of V-ATPases in Cancer. Physiol. Rev 2016, 96 (3), 1071–1091. [PubMed: 27335445]

(30). Armingol E; Officer A; Harismendy O; Lewis NE Deciphering cell–cell interactions and communication from gene expression. Nat. Rev. Genet 2021, 22 (2), 71–88. [PubMed: 33168968]

(31). Chang Y-C; Yang Y-C; Tien C-P; Yang C-J; Hsiao M Roles of Aldolase Family Genes in Human Cancers and Diseases. Trends in Endocrinology & Metabolism 2018, 29 (8), 549–559. [PubMed: 29907340]

(32). Sun M; Chen X; Yang Z Single cell mass spectrometry studies reveal metabolomic features and potential mechanisms of drug-resistant cancer cell lines. Anal. Chim. Acta 2022, 1206, No. 339761. [PubMed: 35473873]

(33). Doan NB; Nguyen HS; Al-Gizawiy MM; Mueller WM; Sabbadini RA; Rand SD; Connelly JM; Chitambar CR; Schmainda KM; Mirza SP Acid ceramidase confers radioresistance to glioblastoma cells. Oncol. Rep 2017, 38 (4), 1932–1940. [PubMed: 28765947]

(34). Tan S-F; Dunton W; Liu X; Fox TE; Morad SA; Desai D; Doi K; Conaway MR; Amin S; Claxton DF; et al. Acid ceramidase promotes drug resistance in acute myeloid leukemia through NF-κB-dependent P-glycoprotein upregulation. Journal of lipid research 2019, 60 (6), 1078–1086. [PubMed: 30962310]

(35). Doan NB; Alhajala H; Al-Gizawiy MM; Mueller WM; Rand SD; Connelly JM; Cochran EJ; Chitambar CR; Clark P; Kuo J; et al. Acid ceramidase and its inhibitors: A de novo drug target and a new class of drugs for killing glioblastoma cancer stem cells with high efficiency. Oncotarget 2017, 8 (68), No. 112662. [PubMed: 29348854]

(36). Aldoghachi AF; Baharudin A; Ahmad U; Chan SC; Ong TA; Yunus R; Razack AH; Yusoff K; Veerakumarasivam A Evaluation of CERS2 Gene as a Potential Biomarker for Bladder Cancer. Dis Markers 2019, 2019, No. 1.

(37). Tian X; Ahsan N; Lulla A; Lev A; Abbosh P; Dicker DT; Zhang S; El-Deiry WS P53-independent partial restoration of the p53 pathway in tumors with mutated p53 through ATF4 transcriptional modulation by ERK1/2 and CDK9. Neoplasia 2021, 23 (3), 304–325. [PubMed: 33582407]

(38). Chesnokova V; Melmed S Pituitary senescence: the evolving role of Pttg. Molecular and cellular endocrinology 2010, 326 (1–2), 55–59. [PubMed: 20153804]

(39). Shah M; Nunes MR; Stearns V CDK4/6 Inhibitors: Game Changers in the Management of Hormone Receptor–Positive Advanced Breast Cancer? Oncology (Williston Park) 2018, 32 (5), 216–22. [PubMed: 29847850]

(40). Cao Y; Li X; Kong S; Shang S; Qi Y CDK4/6 inhibition suppresses tumour growth and enhances the effect of Temozolomide in glioma cells. J. Cell Mol. Med 2020, 24 (9), 5135–5145. [PubMed: 32277580]

(41). Goel S; Bergholz JS; Zhao JJ Targeting CDK4 and CDK6 in cancer. Nature Reviews Cancer 2022, 22 (6), 356–372. [PubMed: 35304604]

(42). Calhoun MW; Thomas JW; Gennis RB The cytochrome oxidase superfamily of redox-driven proton pumps. Trends Biochem. Sci 1994, 19 (8), 325–330. [PubMed: 7940677]

(43). Wilkinson ST; Johnson DBF; Tardif HL; Tome ME; Briehl MM Increased cytochrome c correlates with poor survival in aggressive lymphoma. Oncol Lett. 2010, 1 (2), 227–230. [PubMed: 20798784]

(44). Gomes AP; Ilter D; Low V; Drapela S; Schild T; Mullarky E; Han J; Elia I; Broekaert D; Rosenzweig A; Nagiec M; Nunes JB; Schaffer BE; Mutvei AP; Asara JM; Cantley LC; Fendt S-M; Blenis J Altered propionate metabolism contributes to tumour progression and aggressiveness. Nature Metabolism 2022, 4 (4), 435–443.

(45). Nasgashio R; Sato Y; Matsumoto T; Kageyama T; Iyoda A; Satoh Y; Ryuge S; Masuda N; Jiang S-X; Saegusa M HADHA is a potential predictor of response to platinum-based chemotherapy for lung cancer. Asian Pac J. Cancer Prev 2011, 12 (12), 3457–63. [PubMed: 22471497]

(46). Dewulf JP; Paquay S; Marbaix E; Achouri Y; Van Schaftingen E; Bommer GT ECHDC1 knockout mice accumulate ethyl-branched lipids and excrete abnormal intermediates of branched-chain fatty acid metabolism. J. Biol. Chem 2021, 297 (4), No. 101083. [PubMed: 34419447]

(47). Asai S; Miura N; Sawada Y; Noda T; Kikugawa T; Tanji N; Saika T Silencing of ECHDC1 inhibits growth of gemcitabine-resistant bladder cancer cells. Oncology Letters 2017, 15 (1), 522–527. [PubMed: 29391886]

(48). Shan Y; Gao Y; Jin W; Fan M; Wang Y; Gu Y; Shan C; Sun L; Li X; Yu B; Luo Q; Xu Q Targeting HIBCH to reprogram valine metabolism for the treatment of colorectal cancer. Cell Death & Disease 2019, 10 (8), 618. [PubMed: 31409769]

(49). Levchenko A; Mehta BM; Niu X; Kang G; Villafania L; Way D; Polycarpe D; Sadelain M; Larson SM Intercellular transfer of P-glycoprotein mediates acquired multidrug resistance in tumor cells. Proc. Natl. Acad. Sci. U. S. A 2005, 102 (6), 1933–1938. [PubMed: 15671173]

(50). Wang Y; Zhang L; Wei Y; Huang W; Li L; Wu A.-a.; Dastur A; Greninger P; Bray WM; Zhang C-S; Li M; Lian W; Hu Z; Wang X; Liu G; Yao L; Guh J-H; Chen L; Wang H-R; Zhou D; Lin S-C; Xu Q; Shen Y; Zhang J; Jurica MS; Benes CH; Deng X Pharmacological Targeting of Vacuolar H+-ATPase via Subunit V1G Combats Multidrug-Resistant Cancer. Cell Chemical Biology 2020, 27 (11), 1359–1370. [PubMed: 32649904]

(51). Eniafe J; Jiang S The functional roles of TCA cycle metabolites in cancer. Oncogene 2021, 40 (19), 3351–3363. [PubMed: 33864000]

(52). Wang Z; Zheng W; Chen Z; Wu S; Chang H; Cai M; Cai H Pan-Cancer analysis shows that ACO2 is a potential prognostic and immunotherapeutic biomarker for multiple cancer types including hepatocellular carcinoma. Front Oncol 2022, 12, No. 1055376. [PubMed: 36531056]

(53). Yong L; Tang S; Yu H; Zhang H; Zhang Y; Wan Y; Cai F The role of hypoxia-inducible factor-1 alpha in multidrug-resistant breast cancer. Frontiers in Oncology 2022, 12, No. 964934. [PubMed: 36003773]

(54). Zheng H; Long G; Zheng Y; Yang X; Cai W; He S; Qin X; Liao H Glycolysis-Related SLC2A1 Is a Potential Pan-Cancer Biomarker for Prognosis and Immunotherapy. Cancers 2022, 14 (21), 5344. [PubMed: 36358765]

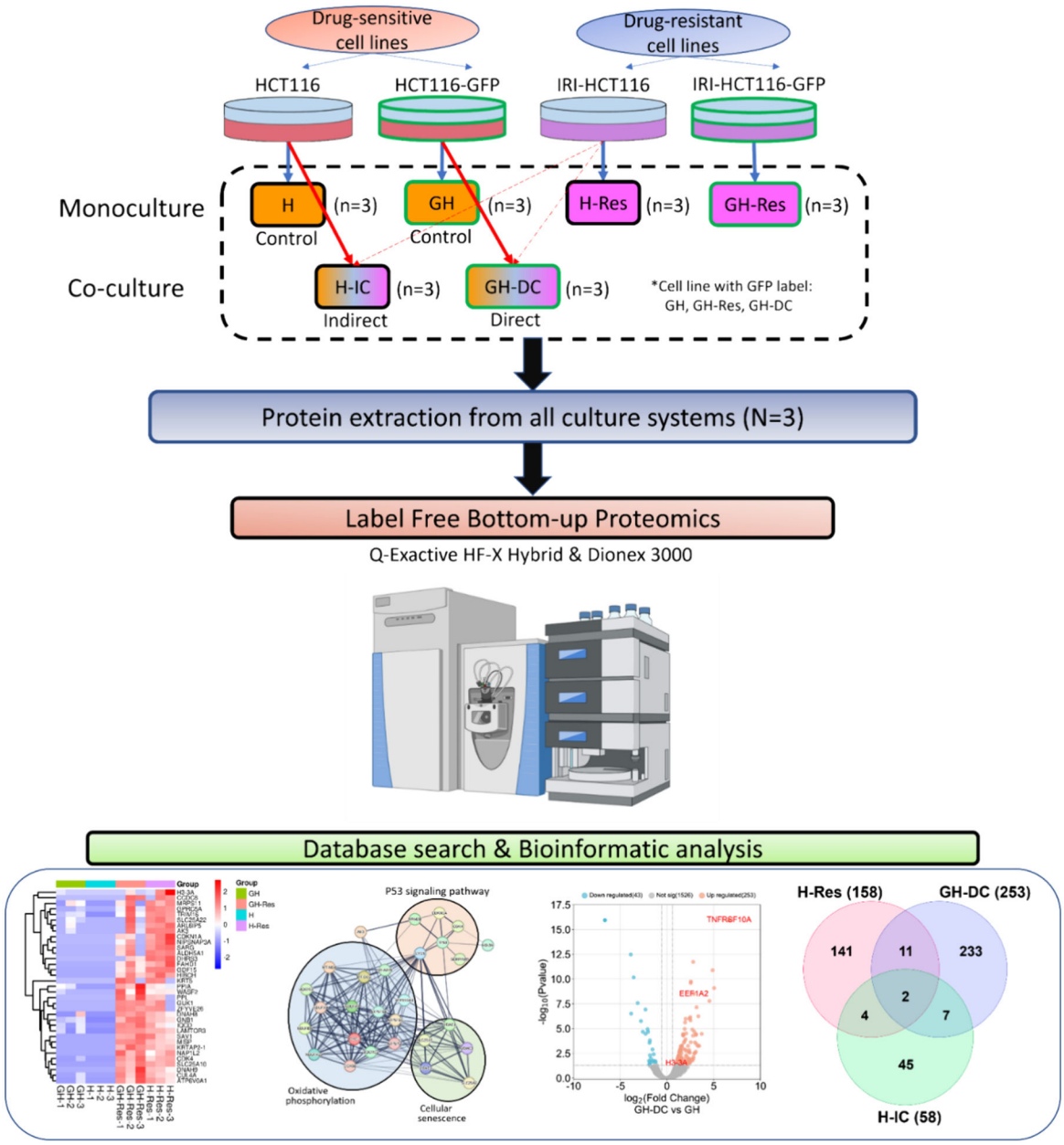

Figure 1.

Flowchart of the experiments and data analysis. Cell lines include HCT116 drug-sensitive cell lines (H and GH), irinotecan-resistant cell lines (H-Res and GH-Res), and drug-sensitive cell lines from indirect coculture (H-IC) and direct coculture (GH-DC).

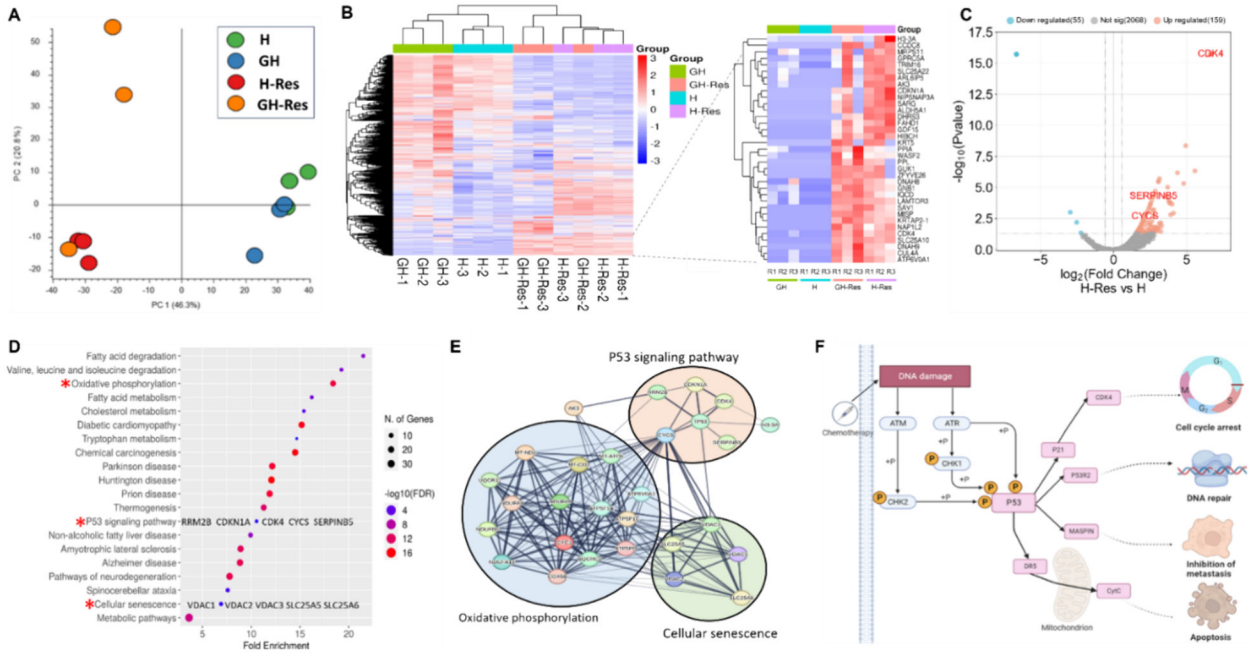

Figure 2.

Bioinformatic analyses of proteins relevant to irinotecan resistance in monoculture cell models. (A) Principal component analysis (PCA) of total proteins in each sample. (B) Heat map clustering of 2,542 unique proteins showing differences between the drug-sensitive (H and GH) and drug-resistant (H-Res and GH-Res) cell groups. (C) Volcano plot analyses of the significantly increased and decreased proteins between two groups. (Fold change > 1.5 or < 0.66 and *p*-value < 0.05). (D) KEEG pathway analysis of all significantly upregulated (fold change > 1.5 and *p*-value < 0.05) proteins in drug-resistant groups. Red asterisks highlight the pathways subjected to protein network analysis using STRING. (E) Upregulated protein networks of the oxidative phosphorylation pathway, cellular senescence, and P53 signaling pathway (from STRING). (F) P53 signaling pathway response after chemotherapy (upregulated proteins are highlighted in pink boxes).

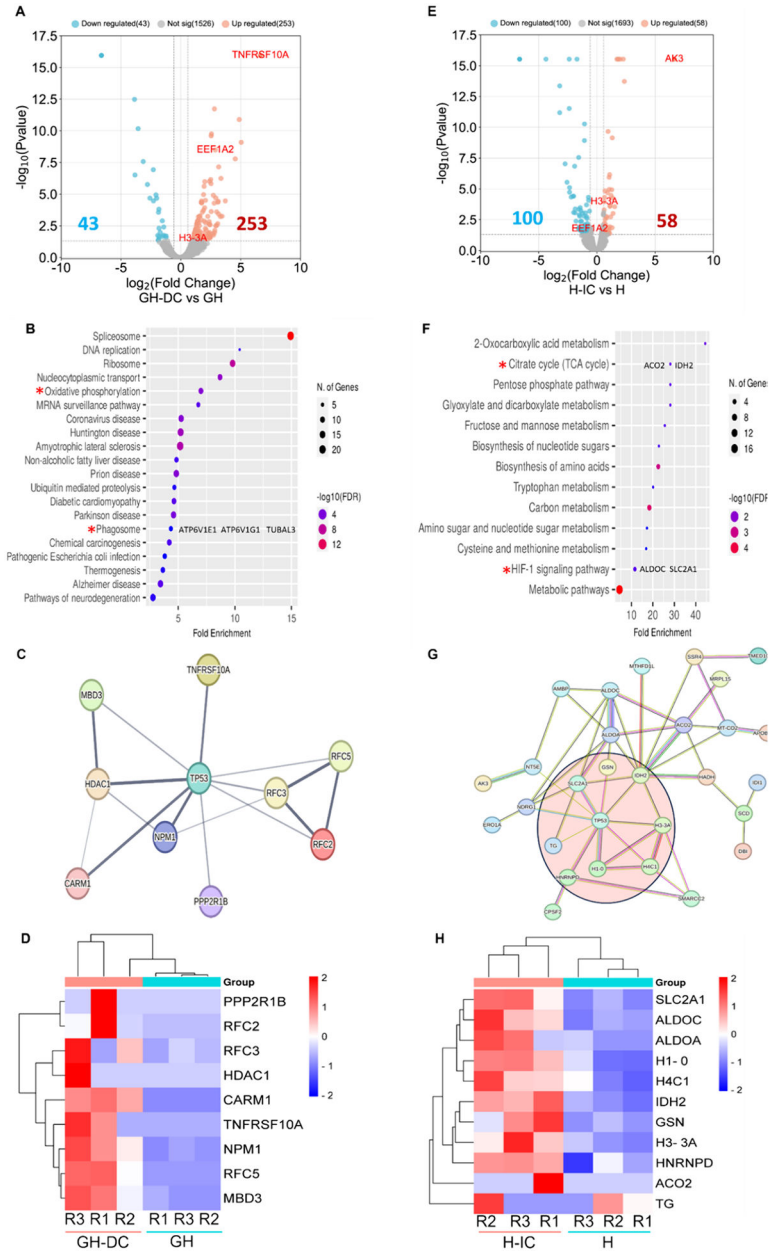

Figure 3.

Bioinformatic analyses of proteomics data obtained from direct (A–D) and indirect coculture (E–H) models. (A and E) Volcano plot of significantly upregulated proteins (p-value < 0.05 and FC > 1.5) in drug-sensitive cells from direct coculture (A) and indirect coculture (E). (B and F) Significantly upregulated pathways in direct coculture (B) and indirect coculture (F). Red asterisks highlight the pathways that are important to these coculture systems: oxidative phosphorylation was found upregulated in drug-resistant cells as well; phagosome shows the activity of those membrane ATP related proteins; and the HIF-1 signaling pathway and TCA cycle proteins have direct interactions with TP53 proteins. (C and G) Upregulated proteins relevant to TP53 pathway transcriptional regulation in direct coculture (C) and indirect coculture (G). (D and H) Heat map of regulated proteins in TP53 transcriptional

regulation in direct coculture (D) and TP53 transcriptional regulation and TCA cycle in indirect coculture (H).

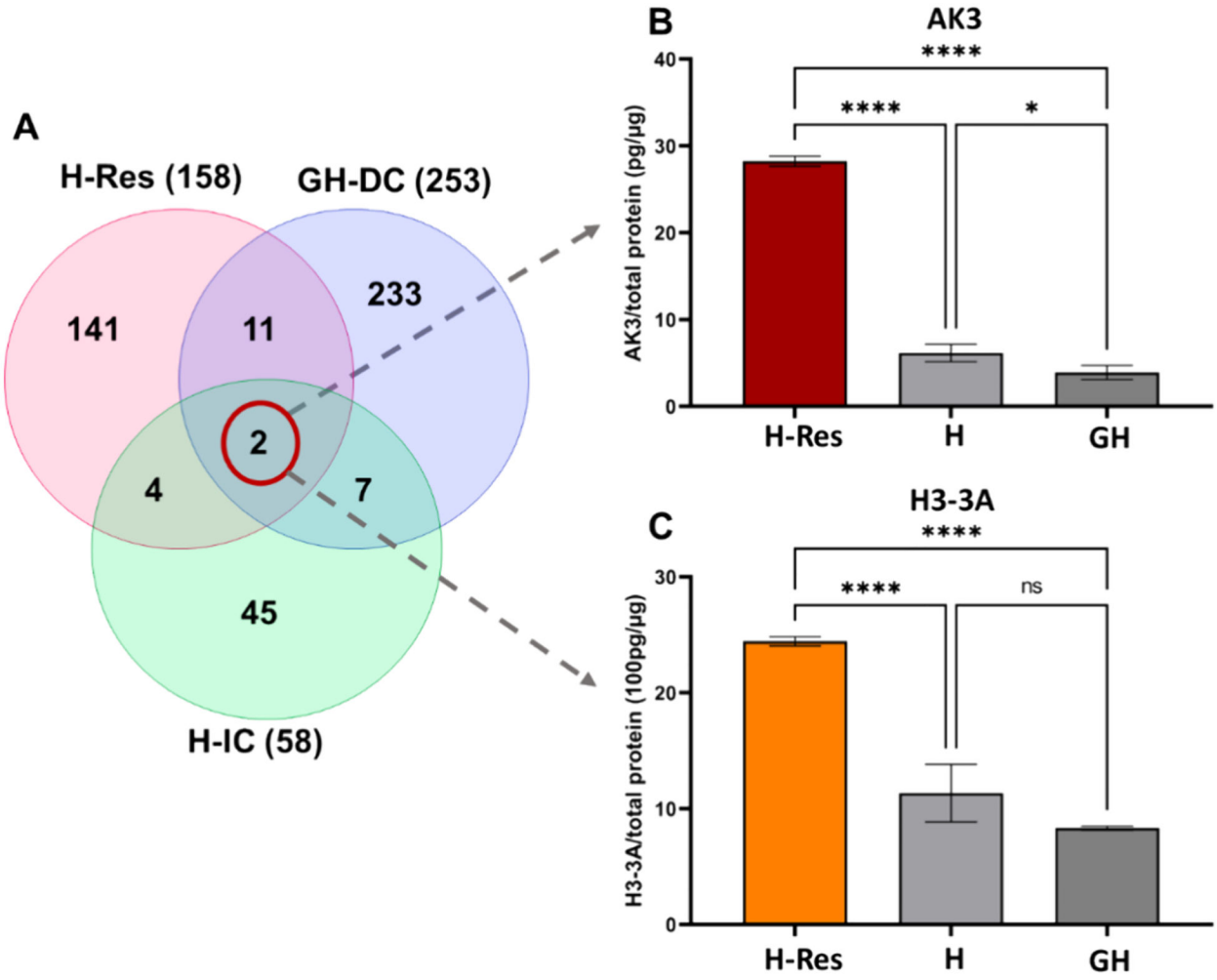

Figure 4.

Significantly upregulated proteins relevant to Iri resistance. (A) Venn diagram of significantly upregulated (FC > 1.5 and *p*-value < 0.05) proteins in direct coculture (GH-DC), indirect coculture (H-IC), and drug-resistant (H-Res) cells. (B and C) ELISA quantification of AK3 (B) and H3–3A (C) proteins in Iri-resistant (H-Res) and control (H and GH) cells. (****p-value < 0.0001; *p-value < 0.05; ns, p-value > 0.05).